

Supplementary information for

**Plasma enhanced anti-coking performance of Pd/CeO₂
catalysts for conversion of methane**

Xiucui Hu,^a Yadi Liu,^a Liguang Dou,^a Cheng Zhang,^{a, b} Shuai Zhang,^{a, b} Yuan Gao,^a Xin
Tu^c and Tao Shao^{a, b *}

^a Beijing International S&T Cooperation Base for Plasma Science and Energy
Conversion, Institute of Electrical Engineering, Chinese Academy of Sciences, Beijing
100190, China

^b University of Chinese Academy of Sciences, Beijing 100049, China

^c Department of Electrical Engineering and Electronics, University of Liverpool,
Liverpool L69 3GJ, United Kingdom

* Corresponding author: st@mail.iee.ac.cn

1. Experimental

1.1 Synthesis of catalysts

CeO₂ supports were synthesized by the reported hydrothermal method.¹ The solution of NaOH (14.4 g, Macklin, 40 mL) and the solution of Ce(NO₃)₂·6H₂O (1.3 g, Macklin, 20 mL) were mixed and stirred for 30 min. Subsequently, the mixed solution was transferred to Teflon-lined stainless-steel autoclaves and heated at 100 °C for 24 h. The precipitates were washed, dried and calcined at 400 °C for 4 h.

The Pd/CeO₂ catalysts were synthesized via a similar deposition-precipitation method.² Typically, appropriate volume of the PdCl₂ aqueous solution (1.0 mg mL⁻¹, Macklin) was added into the aqueous solution including the CeO₂ supports (0.6 g). The pH value was adjusted to ca. 8 by adding a certain volume of NaOH solution (0.2 mol L⁻¹, Macklin). The solids were collected by filtration, dried and calcined in flowing air at 980 °C for 2 h. In this work, the catalysts were denoted as xPd/CeO₂, where *x* is the weight percentage of palladium in ceria.

1.2 Catalytic tests

Methane conversion (*C*_{CH₄}), hydrocarbon products selectivity (*S*_{C_xH_y}) and yields (*Y*_{C_xH_y}), H₂ selectivity (*S*_{H₂}) and yield (*Y*_{H₂}), carbon balances (*B*_C) and hydrogen balances (*B*_H) were calculated according to the following the equations³.

$$C_{\text{CH}_4} (\%) = \frac{\text{moles of CH}_4 \text{ converted}}{\text{moles of initial CH}_4} \times 100 \quad (1)$$

$$S_{\text{C}_x\text{H}_y} (\%) = \frac{x \times \text{moles of C}_x\text{H}_y \text{ produced}}{\text{moles of CH}_4 \text{ converted}} \times 100 \quad (2)$$

$$S_{\text{H}_2} (\%) = \frac{\text{moles of H}_2 \text{ produced}}{2 \times \text{moles of CH}_4 \text{ converted}} \times 100 \quad (3)$$

$$Y_{\text{C}_x\text{H}_y} (\%) = C_{\text{CH}_4} \times S_{\text{C}_x\text{H}_y} \times 100 \quad (4)$$

$$Y_{H_2} (\%) = C_{CH_4} \times S_{H_2} \times 100 \quad (5)$$

$$B_C (\%) = \frac{\text{moles of CH}_4 \text{ unconverted} + \sum_{x=2, 3, 4} x \times \text{moles of C}_x\text{H}_y \text{ produced}}{\text{moles of initial CH}_4} \times 100 \quad (6)$$

$$B_H (\%) = \frac{4 \times \text{moles of CH}_4 \text{ unconverted} + 2 \times \text{moles of H}_2 \text{ produced} + \sum_{y=2, 4, 6, 10} x \times \text{moles of C}_x\text{H}_y \text{ produced}}{4 \times \text{moles of initial CH}_4} \times 100 \quad (7)$$

where the selectivity of C_xH_y product was determined on the basis of carbon balance.

The energy consumption (EC) of the discharge were calculated as follows⁴.

$$EC \text{ (J mmol}^{-1}\text{)} = \frac{P \text{ (J/s)}}{\text{rate of H}_2 \text{ produced (mmol/s)} + \text{rate of C}_x\text{H}_y \text{ produced (mmol/s)}} \quad (8)$$

The discharge power (P) was calculated by the waveforms of discharge voltage and discharge current. Here, we think the external power of the furnace to be the same under the same discharge conditions and constant temperature. Thus, in our work, only the discharge power of the plasma was considered.

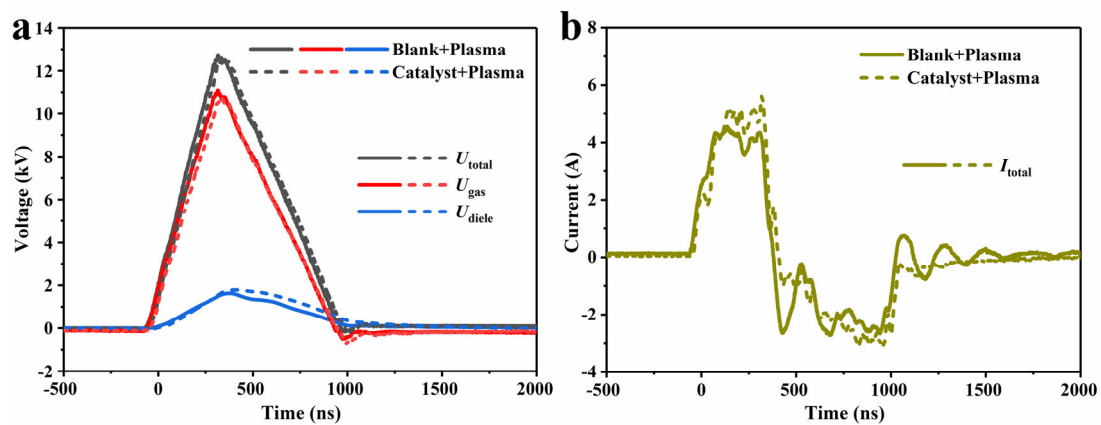


Figure S1. (a) Typical voltage waveforms and (b) typical current waveforms over the 0.5Pd/CeO₂ catalyst in comparison to that over a blank reactor with plasma at 980 °C (discharge voltage: 13 kV; frequency: 3 kHz; rising time: 300 ns; falling time: 500 ns).

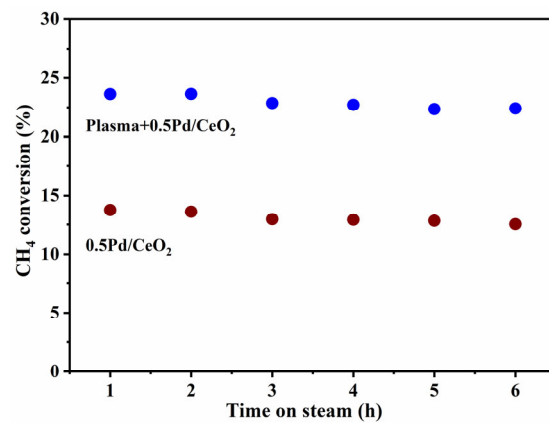


Figure S2. The stability of the catalysts at 980 °C under both thermal and plasma conditions for 6 h.

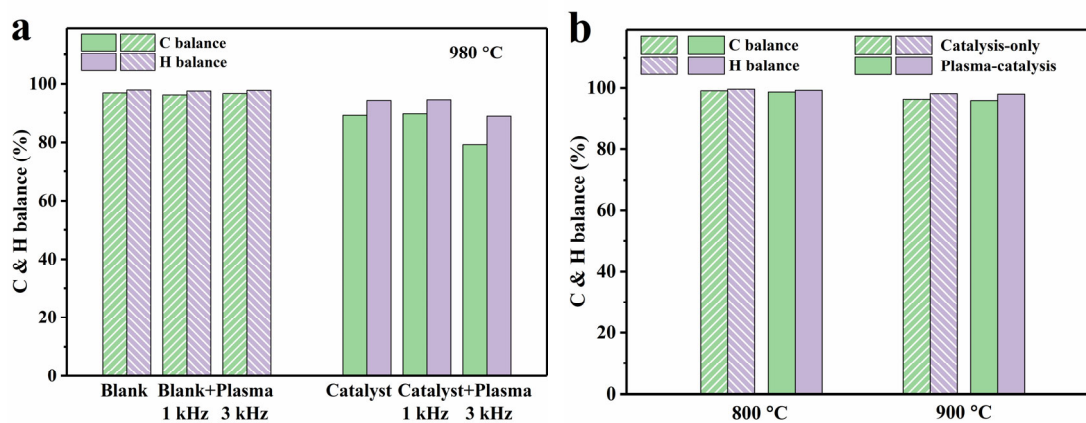


Figure S3. (a) C & H balance over the 0.5Pd/CeO₂ catalyst in comparison to that over a blank reactor with or without plasma at 980 °C (discharge voltage: 13 kV; frequency: 1 kHz or 3 kHz; rising time: 300 ns; falling time: 500 ns). (b) C & H balance over the 0.5Pd/CeO₂ catalyst with or without plasma at 800 °C and 900 °C (discharge voltage: 13 kV; frequency: 1 kHz; rising time: 300 ns; falling time: 500 ns).

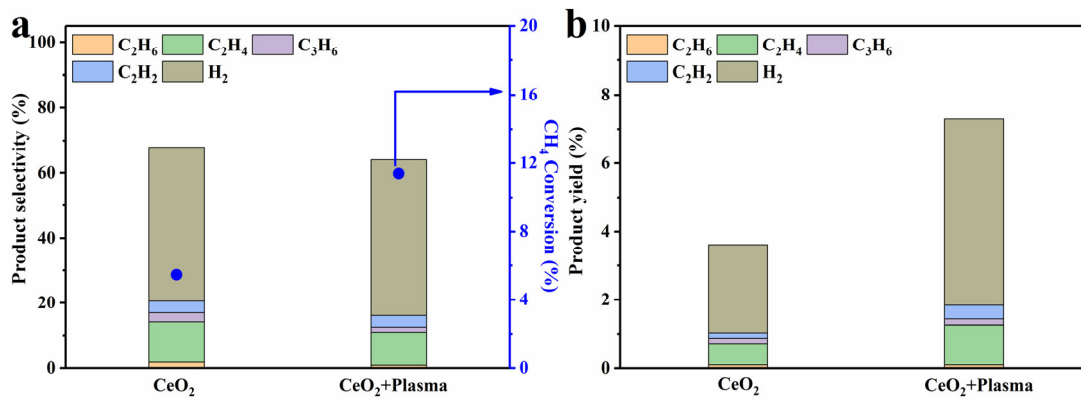


Figure S4. (a) Methane conversion, product selectivity and (b) product yield over the CeO₂ support with or without plasma at 980 °C (discharge voltage: 13 kV; frequency: 3 kHz; rising time: 300 ns; falling time: 500 ns).

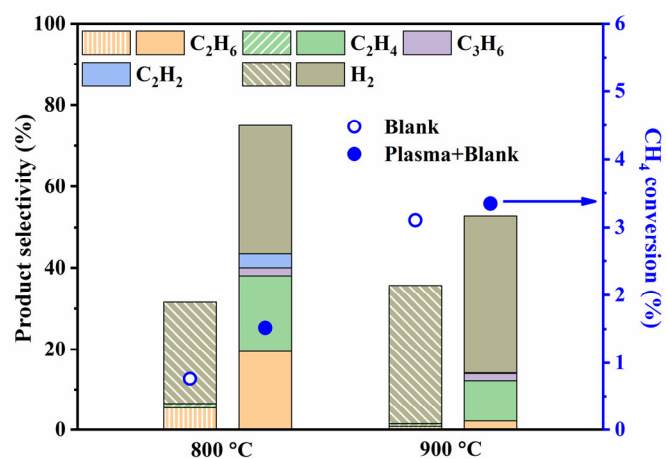


Figure S5. Methane conversion and product selectivity over the blank reactor without catalysts in the presence and absence of plasma at different temperatures.

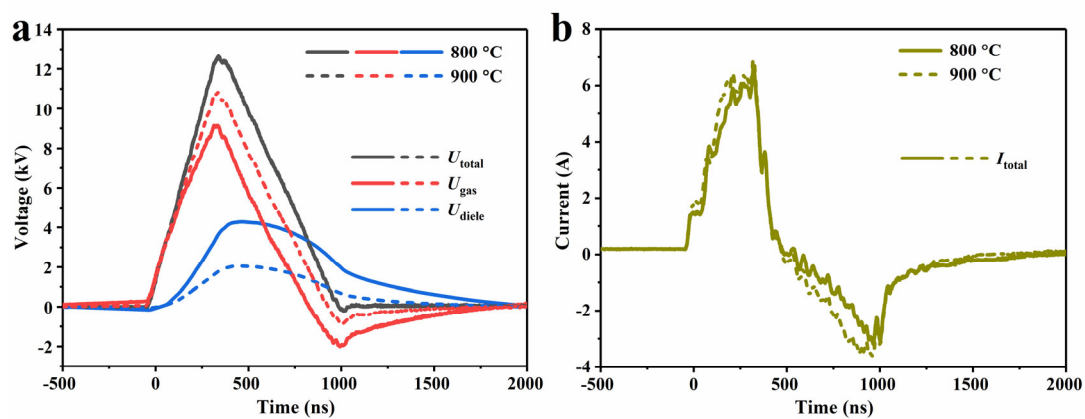


Figure S6. (a) Typical voltage waveforms and (b) typical current waveforms over the 0.5Pd/CeO₂ catalyst with plasma at 800 °C and 900 °C (discharge voltage: 13 kV; frequency: 1 kHz; rising time: 300 ns; falling time: 500 ns).

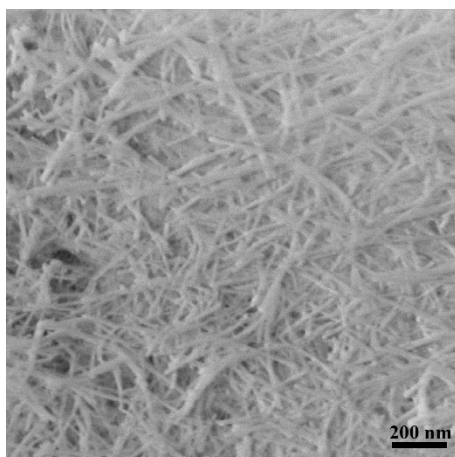


Figure S7. SEM image of the CeO₂ support calcined at 400 °C.

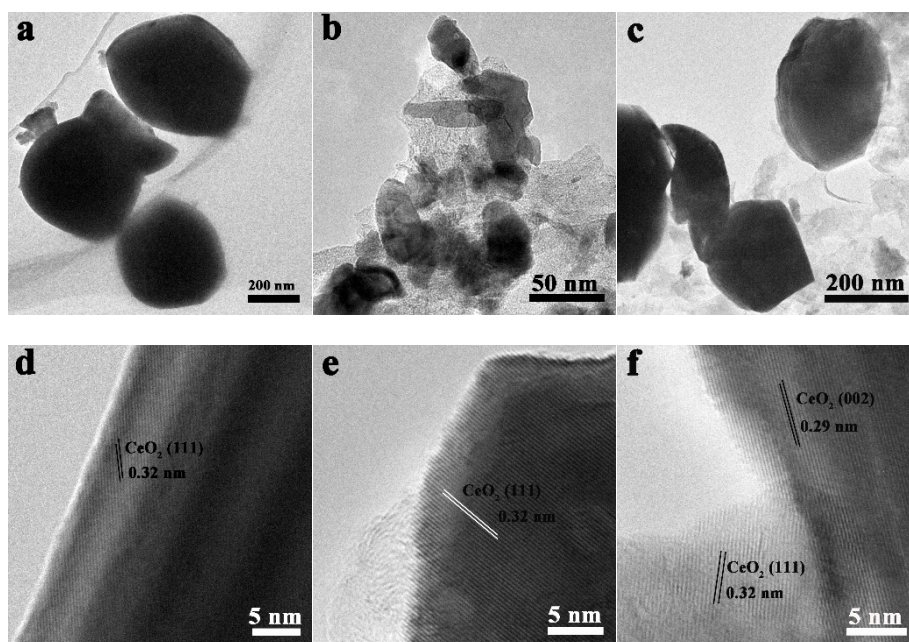


Figure S8. (a–c) TEM images, (d–f) HRTEM images for the 0.5Pd/CeO₂ catalysts: (a, d) the fresh catalyst calcined at 980 °C; (b, e) the catalyst after catalysis-only at 980 °C; (c, f) the catalyst after plasma-catalysis at 980 °C.

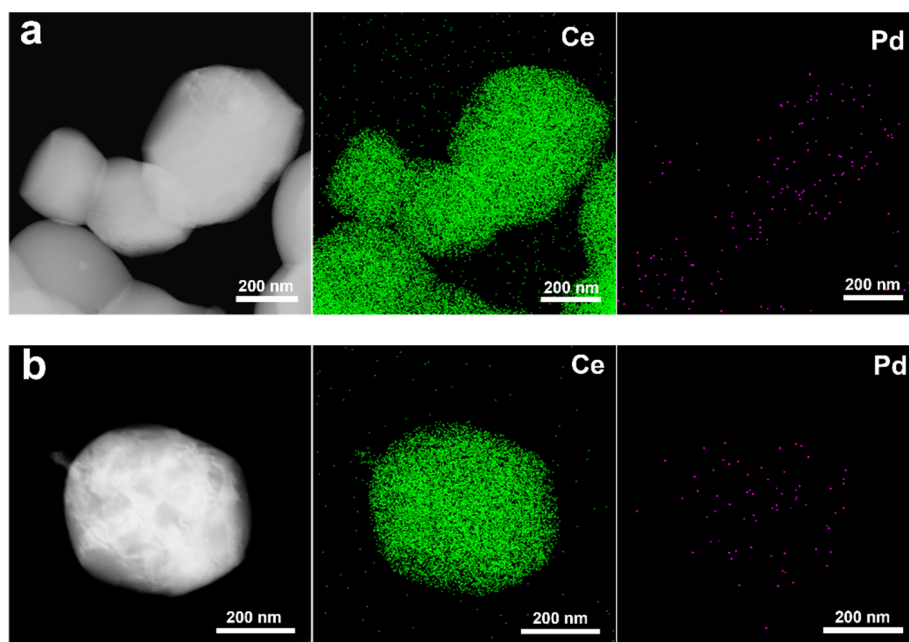


Figure S9. HAADF-STEM images and elemental mappings of the catalysts: (a) the fresh 0.5Pd/CeO₂ calcined at 980 °C; (b) the used 0.5Pd/CeO₂ under plasma-catalysis condition at 980 °C.

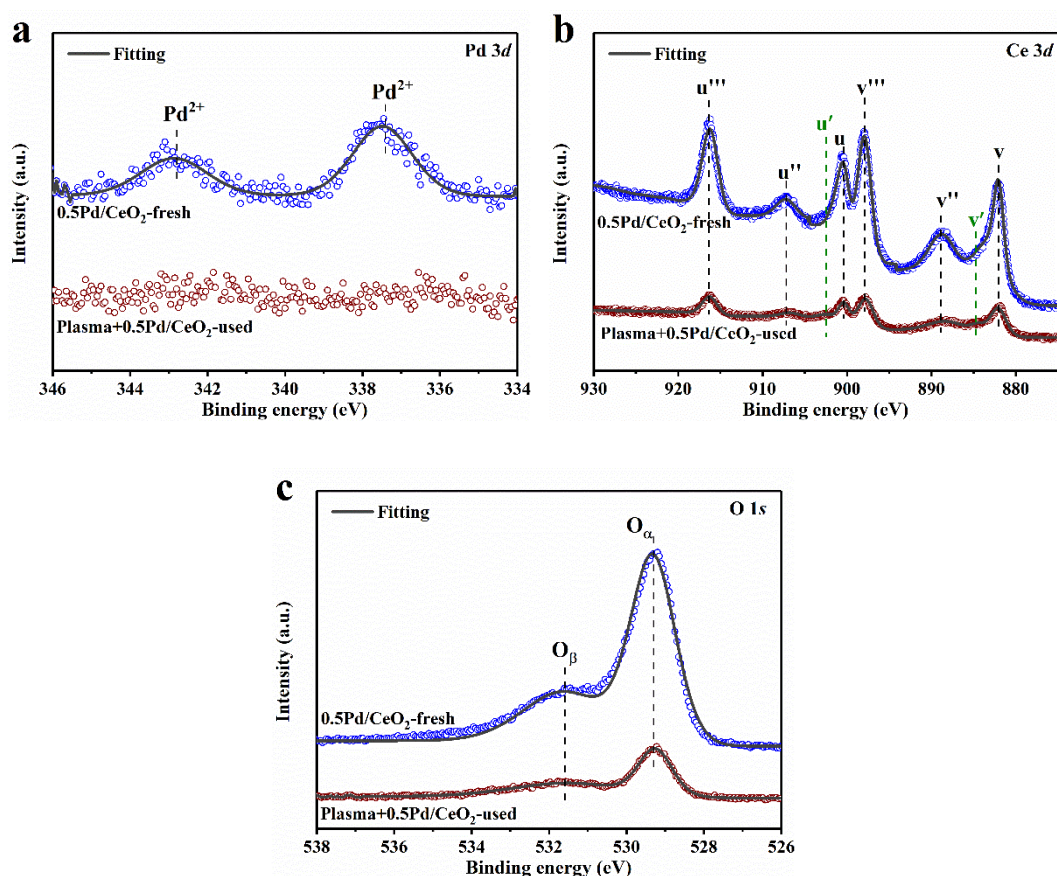


Figure S10. XPS spectra of Pd 3d (a), Ce 3d (b) and O 1s (c) for the fresh 0.5Pd/CeO₂ catalyst and the used Plasma+0.5Pd/CeO₂ catalyst.

For the XPS spectrum of Ce 3d (Figure S10b), six peaks denoted as v (882.0 eV), v'' (888.7 eV), v''' (897.9 eV), u (900.3 eV), u'' (907.2 eV), u''' (916.2 eV) were attributed to Ce⁴⁺.^{5,6} Another two peaks denoted as v' (883.1 eV) and u' (902.4 eV) were assigned to Ce³⁺.^{5,6} For the XPS spectrum of O 1s (Figure S10c), two peaks at 529.7 eV and 531.9 eV were assigned to lattice oxygen (denoted as O_α) in the ceria and the adsorbed oxygen or oxygen in hydroxyl-like groups (denoted as O_β) on the catalyst surface,^{5,6} respectively. After the CH₄ conversion, the XPS spectra of Ce 3d and O 1s in intensity were much lower compared with those before the reaction (Figure S10b, c), demonstrating the coverage of carbon species on 0.5Pd/CeO₂.

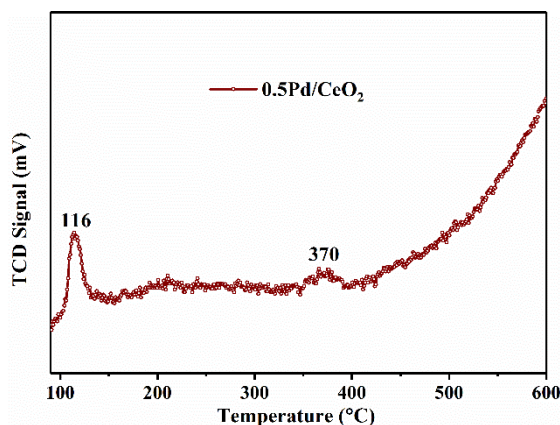


Figure S11. H₂-TPR profile of the fresh 0.5Pd/CeO₂ catalysts.

H₂-TPR measurement was used to investigate the reducibility of 0.5Pd/CeO₂. As shown in Figure S11, the first reduction peak (at ca. 116 °C) can be assigned to the reduction of highly dispersed PdO.^{7, 8} The reduction peak (at above 300 °C) can be related to the reduction of stable PdO species interacting strongly with CeO₂^{7, 8} and the reduction of the oxygen in ceria.^{10, 11}

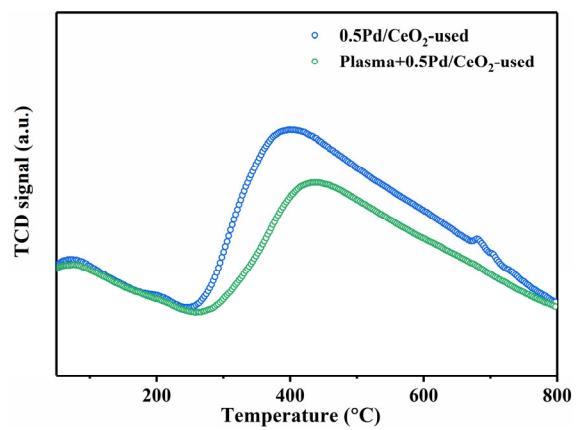


Figure S12. O₂-TPO profiles of the used 0.5Pd/CeO₂ and Plasma+0.5Pd/CeO₂.

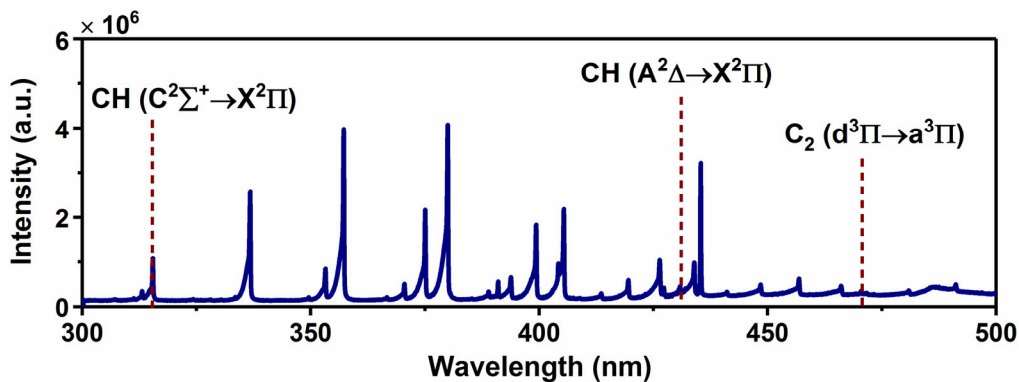


Figure S13. Typical optical emission spectra during the conversion of CH₄ under the plasma-catalysis condition.

The OES measurement was used to detect the active species during the plasma-catalysis conditions. Two peaks at 315.5 nm and 431.0 nm were assigned to the vibrational-rotational bands of CH ($C^2\Sigma^+ \rightarrow X^2\Pi$) and CH ($A^2\Delta \rightarrow X^2\Pi$),^{12, 13} respectively. The peak at 471.5 nm was attributed to the C₂ ($d^3\Pi \rightarrow a^3\Pi$) bands.^{12, 13}

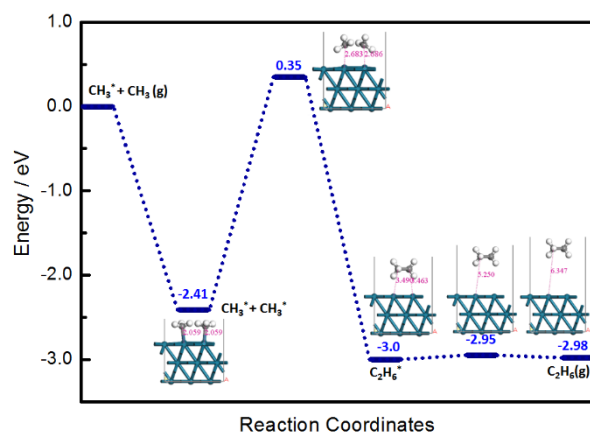


Figure S14. The DFT simulations of the CH₃ radicals reacting with the adsorbed CH₃ on Pd-site.

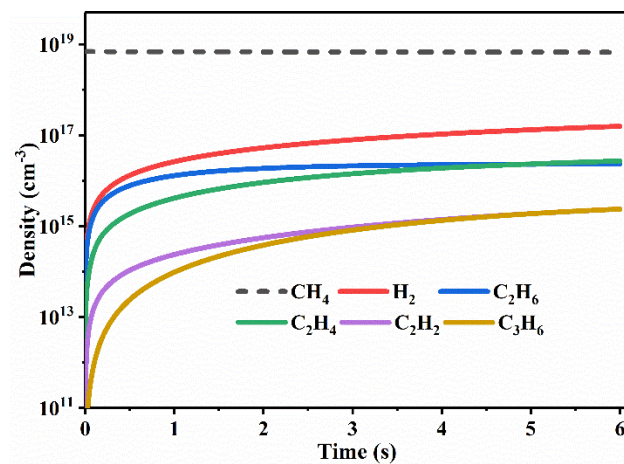


Figure S15. The density of the CH₄ and main products as a function of time for the CH₄ conversion assisted by plasma without catalyst.

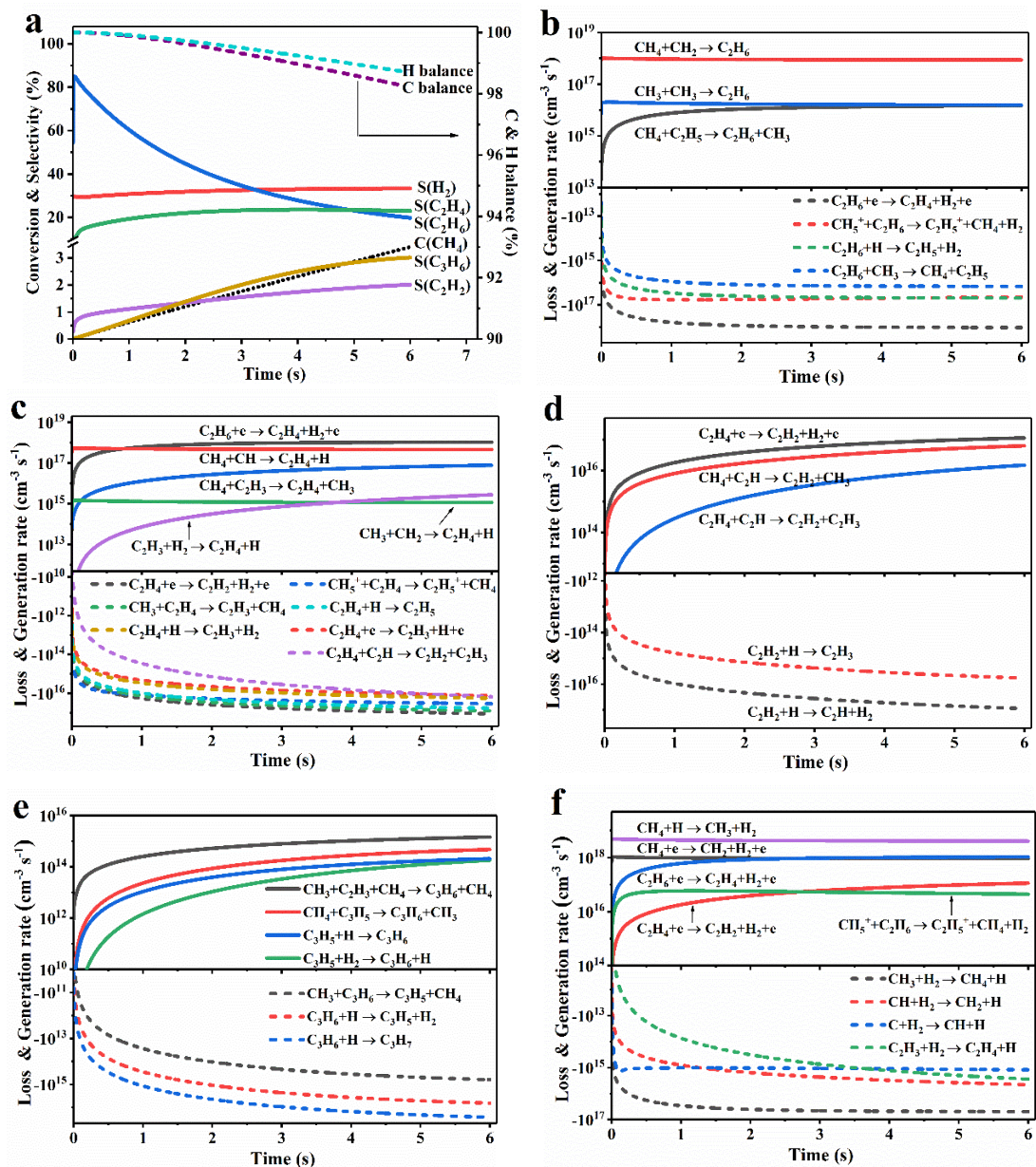


Figure S16. (a) CH₄ conversion, selectivity of major products and C & H balance as a function of time for the CH₄ conversion assisted by plasma without catalyst. (b–f) Generation and loss rates of the products as a function of time for the CH₄ conversion: (b) C₂H₆, (c) C₂H₄, (d) C₂H₂, (e) C₃H₆, (f) H₂.

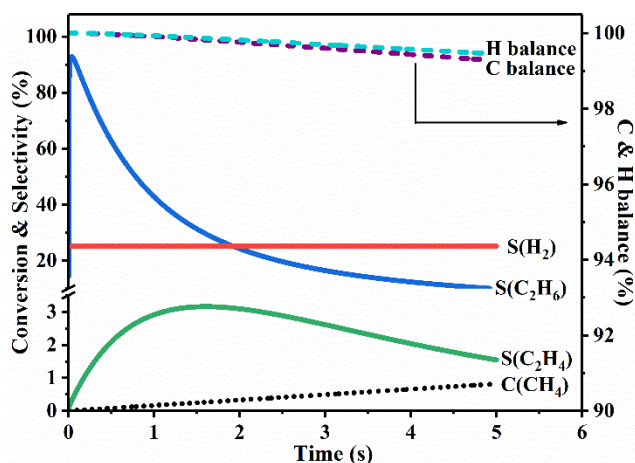


Figure S17. CH₄ conversion, selectivity of major products and C & H equilibrium as a function of time for the CH₄ conversion in the blank reactor without catalyst and plasma.

The main formation pathway of C₂H₆ was $\text{CH}_3 + \text{CH}_3 \rightarrow \text{C}_2\text{H}_6$ (R41, Table S1) and the main consumption pathway was the continuous generation of the high-carbon alkanes or the polymerization by olefins or alkyne, namely, $\text{C}_2\text{H}_6 \rightarrow \text{M}$ (R132, Table S1, M is liquid or solid substances). The main generation pathway of C₂H₄ was $\text{C}_2\text{H}_3 + \text{CH}_4 \rightarrow \text{CH}_3 + \text{C}_2\text{H}_4$ (R33, Table S1), and the main consumption pathway was its reverse reaction (R46, Table S1). The main reaction pathway to produce H₂ was $\text{CH}_4 + \text{H} \rightarrow \text{CH}_3 + \text{H}_2$ (R37, Table S1) and the main consumption pathway was also its reverse reaction (R53, Table S1). Similarly, the CH₄ conversion, selectivity of major products and C & H balance at 4.8 s was calculated and compared with the experimental results (Table S5), verifying the reliability of the CH₄ thermal cracking model.

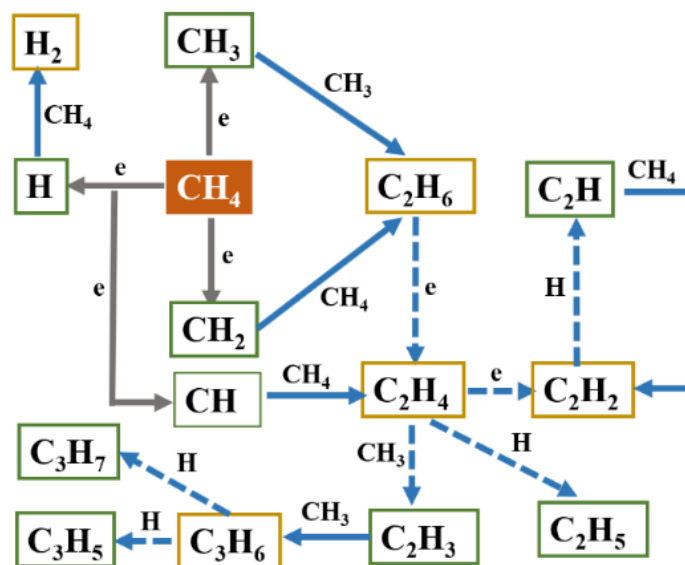


Figure S18. Possible reaction pathways for the CH₄ conversion assisted by plasma without catalyst.

Table S1. Plasma chemistry involved in this model.

No.	Reaction	Rate coefficient ^a	Reference
<i>Electron-neutral reactions^b</i>			
R1	CH ₄ +e→CH ₃ +H+e	Bolsig+	14
R2	CH ₄ +e→CH ₂ +H ₂ +e	Bolsig+	14
R3	CH ₄ +e→CH+3H+e	Bolsig+	14
R4	CH ₄ +e→C+4H+e	Bolsig+	14
R5	CH ₄ +e→CH ₄ ⁺ +2e	Bolsig+	14
R6	CH ₄ +e→CH ₃ ⁺ +H+2e	Bolsig+	14
R7	C ₂ H ₄ +e→C ₂ H ₂ +H ₂ +e	Bolsig+	15
R8	C ₂ H ₄ +e→C ₂ H ₃ +H+e	Bolsig+	15
R9	C ₂ H ₆ +e→C ₂ H ₅ +H+e	Bolsig+	15
R10	C ₂ H ₆ +e→C ₂ H ₄ +H ₂ +e	Bolsig+	15
R11	C ₃ H ₆ +e→C ₂ H ₂ +CH ₄ +e	Bolsig+	15
R12	C ₃ H ₈ +e→C ₃ H ₆ +H ₂ +e	Bolsig+	15
R13	C ₃ H ₈ +e→C ₂ H ₄ +CH ₄ +e	Bolsig+	15
<i>Electron-ion reactions</i>			
R14	CH ₅ ⁺ +e→CH ₃ +2H	$2.57 \times 10^{-7} \times (300/T_g)^{0.3}$	16
R15	CH ₅ ⁺ +e→CH ₂ +H ₂ +H	$6.61 \times 10^{-8} \times (300/T_g)^{0.3}$	16
R16	CH ₄ ⁺ +e→CH ₃ +H	$1.18 \times 10^{-8} \times (300/T_g)^{0.5}$	16
R17	CH ₄ ⁺ +e→CH ₂ +2H	$2.42 \times 10^{-8} \times (300/T_g)^{0.5}$	16
R18	CH ₄ ⁺ +e→CH+H ₂ +H	$1.41 \times 10^{-8} \times (300/T_g)^{0.5}$	14
R19	CH ₃ ⁺ +e→CH ₂ +H	$2.25 \times 10^{-8} \times (300/T_g)^{0.5}$	16
R20	CH ₃ ⁺ +e→CH+H ₂	$7.88 \times 10^{-9} \times (300/T_g)^{0.5}$	16
R21	CH ₃ ⁺ +e→CH+2H	$9 \times 10^{-9} \times (300/T_g)^{0.5}$	16
R22	CH ₃ ⁺ +e→C+H ₂ +H	$1.69 \times 10^{-8} \times (300/T_g)^{0.5}$	16
R23	C ₂ H ₅ ⁺ +e→C ₂ H ₃ +2H	$1.92 \times 10^{-8} \times (300/T_g)^{0.71}$	15
R24	C ₂ H ₅ ⁺ +e→C ₂ H ₂ +3H	$8.98 \times 10^{-9} \times (300/T_g)^{0.71}$	15
R25	C ₂ H ₅ ⁺ +e→C ₂ H ₂ +H ₂ +H	$1.6 \times 10^{-8} \times (300/T_g)^{0.71}$	15
<i>Ion-neutral reactions</i>			
R26	CH ₄ ⁺ +CH ₄ →CH ₅ ⁺ +CH ₃	1.5×10^{-9}	16
R27	CH ₃ ⁺ +CH ₄ →C ₂ H ₅ ⁺ +H ₂	1.2×10^{-9}	16
R28	CH ₅ ⁺ +C ₂ H ₄ →C ₂ H ₅ ⁺ +CH ₄	1.5×10^{-9}	16
R29	CH ₅ ⁺ +C ₂ H ₆ →C ₂ H ₅ ⁺ +CH ₄ +H ₂	2.25×10^{-10}	16
<i>Neutral-neutral reactions (b)</i>			
R30	CH ₄ +CH ₂ →CH ₃ +CH ₃	$4.08 \times 10^{-18} T_g^2 \exp(-4163/T_g)$	16
R31	CH ₄ +CH→C ₂ H ₄ +H	9.97×10^{-11}	16
R32	CH ₄ +C ₂ H ₅ →C ₂ H ₆ +CH ₃	$2.51 \times 10^{-15} (T_g/298)^{4.14} \exp(-52.55/R/T_g)$	16
R33	CH ₄ +C ₂ H ₃ →C ₂ H ₄ +CH ₃	$4.26 \times 10^{-15} (T_g/298)^{4.02} \exp(-22.86/R/T_g)$	16
R34	CH ₄ +C ₂ H→C ₂ H ₂ +CH ₃	$3.01 \times 10^{-12} \exp(-2.08/R/T_g)$	16
R35	CH ₄ +C ₃ H ₇ →C ₃ H ₈ +CH ₃	$3.54 \times 10^{-16} (T_g/298)^{4.02} \exp(-45.48/R/T_g)$	16
R36	CH ₄ +C ₃ H ₅ →C ₃ H ₆ +CH ₃	$1.71 \times 10^{-14} (T_g/298)^{3.4} \exp(-97.28/R/T_g)$	16
R37	CH ₄ +H→CH ₃ +H ₂	$9.86 \times 10^{-13} (T_g/298)^3 \exp(-36.67/R/T_g)$	16

R38	$\text{CH}_4+\text{CH}_3\rightarrow\text{H}+\text{C}_2\text{H}_6$	$1.33\times 10^{-10} \exp(-167/R/T_g)$	16
R39	$\text{CH}_4+\text{CH}_2\rightarrow\text{C}_2\text{H}_6$	1.9×10^{-12}	16
R40	$\text{CH}_3+\text{CH}_3\rightarrow\text{C}_2\text{H}_5+\text{H}$	$5\times 10^{-11} \exp(-56.54/R/T_g)$	16
R41	$\text{CH}_3+\text{CH}_3\rightarrow\text{C}_2\text{H}_6$	$1.12\times 10^{-7} T_g^{-1.18} \exp(-329.14/T_g)$	16
R42	$\text{CH}_3+\text{CH}_2\rightarrow\text{C}_2\text{H}_4+\text{H}$	7.1×10^{-11}	16
R43	$\text{CH}_3+\text{C}_2\text{H}_6\rightarrow\text{C}_2\text{H}_5+\text{CH}_4$	$7.19\times 10^{-15} (T_g/298)^4 \exp(-34.67/R/T_g)$	16
R44	$\text{CH}_3+\text{C}_2\text{H}_5\rightarrow\text{C}_2\text{H}_4+\text{CH}_4$	1.91×10^{-12}	16
R45	$\text{CH}_3+\text{C}_2\text{H}_5\rightarrow\text{C}_3\text{H}_8$	1.56×10^{-11}	16
R46	$\text{CH}_3+\text{C}_2\text{H}_4\rightarrow\text{C}_2\text{H}_3+\text{CH}_4$	$2.18\times 10^{-11} \exp(-46.56/R/T_g)$	16
R47	$\text{CH}_3+\text{C}_2\text{H}_3\rightarrow\text{C}_2\text{H}_2+\text{CH}_4$	$1.5\times 10^{-11} \exp(3.2/R/T_g)$	16
R48	$\text{CH}_3+\text{C}_2\text{H}_3+\text{CH}_4\rightarrow\text{C}_3\text{H}_6+\text{CH}_4$	3.8×10^{-29}	16
R49	$\text{CH}_3+\text{C}_2\text{H}_2\rightarrow\text{CH}_4+\text{C}_2\text{H}$	$3\times 10^{-13} \exp(-72.34/R/T_g)$	16
R50	$\text{CH}_3+\text{C}_3\text{H}_8\rightarrow\text{C}_3\text{H}_7+\text{CH}_4$	$1.5\times 10^{-24} T_g^{3.65} \exp(-3600.4/T_g)$	16
R51	$\text{CH}_3+\text{C}_3\text{H}_7\rightarrow\text{C}_3\text{H}_6+\text{CH}_4$	$3.07\times 10^{-12} (T_g/298)^{-0.32}$	16
R52	$\text{CH}_3+\text{C}_3\text{H}_6\rightarrow\text{C}_3\text{H}_5+\text{CH}_4$	$1.68\times 10^{-15} (T_g/298)^{3.5} \exp(-23.78/R/T_g)$	16
R53	$\text{CH}_3+\text{H}_2\rightarrow\text{CH}_4+\text{H}$	$2.52\times 10^{-14} (T_g/298)^{3.12} \exp(-36.42/R/T_g)$	16
R54	$\text{CH}_3+\text{H}\rightarrow\text{CH}_2+\text{H}_2$	$1\times 10^{-10} \exp(-63.19/R/T_g)$	16
R55	$\text{CH}_3+\text{H}\rightarrow\text{CH}_4$	$2.31\times 10^{-8} T_g^{-0.534} \exp(-269.75/T_g)$	16
R56	$\text{CH}_2+\text{CH}_2\rightarrow\text{C}_2\text{H}_2+2\text{H}$	$3.32\times 10^{-10} \exp(-45.98/R/T_g)$	16
R57	$\text{CH}_2+\text{C}_2\text{H}_5\rightarrow\text{C}_2\text{H}_4+\text{CH}_3$	3.01×10^{-11}	16
R58	$\text{CH}_2+\text{C}_2\text{H}_3\rightarrow\text{C}_2\text{H}_2+\text{CH}_3$	3.01×10^{-11}	16
R59	$\text{CH}_2+\text{C}_2\text{H}\rightarrow\text{C}_2\text{H}_2+\text{CH}$	3.01×10^{-11}	16
R60	$\text{CH}_2+\text{C}_3\text{H}_8\rightarrow\text{C}_3\text{H}_7+\text{CH}_3$	$1.61\times 10^{-15} (T_g/298)^{3.65} \exp(-29.93/R/T_g)$	16
R61	$\text{CH}_2+\text{C}_3\text{H}_7\rightarrow\text{C}_2\text{H}_4+\text{C}_2\text{H}_5$	3.01×10^{-11}	16
R62	$\text{CH}_2+\text{C}_3\text{H}_7\rightarrow\text{C}_3\text{H}_6+\text{CH}_3$	3.01×10^{-11}	16
R63	$\text{CH}_2+\text{C}_3\text{H}_6\rightarrow\text{C}_3\text{H}_5+\text{CH}_3$	$1.2\times 10^{-12} \exp(-25.94/R/T_g)$	16
R64	$\text{CH}_2+\text{H}_2\rightarrow\text{CH}_3+\text{H}$	$8.3\times 10^{-19} T_g^2 \exp(-3938.65/T_g)$	16
R65	$\text{CH}_2+\text{H}\rightarrow\text{CH}+\text{H}_2$	$1\times 10^{-11} \exp(7.48/R/T_g)$	16
R66	$\text{CH}+\text{C}_2\text{H}_6+\text{CH}_4\rightarrow\text{C}_3\text{H}_7+\text{CH}_4$	1.14×10^{-29}	16
R67	$\text{CH}+\text{H}_2\rightarrow\text{CH}_2+\text{H}$	$1.79\times 10^{-10} \exp(-1565.17/T_g)$	16
R68	$\text{CH}+\text{H}\rightarrow\text{C}+\text{H}_2$	4.98×10^{-11}	16
R69	$\text{CH}+\text{CH}_3\rightarrow\text{C}_2\text{H}_3+\text{H}$	4.98×10^{-11}	16
R70	$\text{CH}+\text{CH}_2\rightarrow\text{C}_2\text{H}_2+\text{H}$	6.64×10^{-11}	16
R71	$\text{CH}+\text{C}_2\text{H}_3\rightarrow\text{CH}_2+\text{C}_2\text{H}_2$	8.3×10^{-11}	16
R72	$\text{C}+\text{H}_2\rightarrow\text{CH}+\text{H}$	$6.64\times 10^{-10} \exp(-97.28/R/T_g)$	16
R73	$\text{C}_2\text{H}_6+\text{C}_2\text{H}_3\rightarrow\text{C}_2\text{H}_5+\text{C}_2\text{H}_4$	$1.46\times 10^{-13} (T_g/298)^{3.3} \exp(-43.9/R/T_g)$	16
R74	$\text{C}_2\text{H}_6+\text{C}_2\text{H}\rightarrow\text{C}_2\text{H}_2+\text{C}_2\text{H}_5$	5.99×10^{-12}	16
R75	$\text{C}_2\text{H}_6+\text{C}_3\text{H}_7\rightarrow\text{C}_3\text{H}_8+\text{C}_2\text{H}_5$	$1.19\times 10^{-15} (T_g/298)^{3.82} \exp(-37.83/R/T_g)$	16
R76	$\text{C}_2\text{H}_6+\text{C}_3\text{H}_5\rightarrow\text{C}_3\text{H}_6+\text{C}_2\text{H}_5$	$5.71\times 10^{-14} (T_g/298)^{3.3} \exp(-83.06/R/T_g)$	16
R77	$\text{C}_2\text{H}_6+\text{H}\rightarrow\text{C}_2\text{H}_5+\text{H}_2$	$1.23\times 10^{-11} (T_g/298)^{1.5} \exp(-31.01/R/T_g)$	16
R78	$2\text{C}_2\text{H}_5\rightarrow\text{C}_2\text{H}_6+\text{C}_2\text{H}_4$	2.41×10^{-12}	16
R79	$\text{C}_2\text{H}_5+\text{C}_2\text{H}_4\rightarrow\text{C}_2\text{H}_6+\text{C}_2\text{H}_3$	$5.83\times 10^{-14} (T_g/298)^{3.13} \exp(-75.33/R/T_g)$	16
R80	$\text{C}_2\text{H}_5+\text{C}_2\text{H}_2\rightarrow\text{C}_2\text{H}_6+\text{C}_2\text{H}$	$4.5\times 10^{-13} \exp(-98.11/R/T_g)$	16

R81	$C_2H_5+C_2H \rightarrow C_2H_4+C_2H_2$	3.01×10^{-12}	16
R82	$C_2H_5+C_3H_8 \rightarrow C_2H_6+C_3H_7$	$1.61 \times 10^{-15} (T_g/298)^{3.65} \exp(-38.25/R/T_g)$	16
R83	$C_2H_5+C_3H_7 \rightarrow C_3H_8+C_2H_4$	1.91×10^{-12}	16
R84	$C_2H_5+C_3H_7 \rightarrow C_3H_6+C_2H_6$	2.41×10^{-12}	16
R85	$C_2H_5+C_3H_6 \rightarrow C_3H_5+C_2H_6$	$1.69 \times 10^{-15} (T_g/298)^{3.5} \exp(-35.34/R/T_g)$	16
R86	$C_2H_5+C_3H_5 \rightarrow C_3H_6+C_2H_4$	5.36×10^{-12}	16
R87	$C_2H_5+H_2 \rightarrow C_2H_6+H$	$4.12 \times 10^{-15} (T_g/298)^{3.6} \exp(-27.77/R/T_g)$	16
R88	$C_2H_5+H \rightarrow 2CH_3$	5.99×10^{-11}	16
R89	$C_2H_5+H \rightarrow C_2H_4+H_2$	3.32×10^{-12}	16
R90	$C_2H_5+H \rightarrow C_2H_6$	$8.65 \times 10^{-7} T_g^{-0.99} \exp(-795.17/T_g)$	16
R91	$C_2H_4+C_2H \rightarrow C_2H_2+C_2H_3$	1.4×10^{-10}	16
R92	$C_2H_4+H \rightarrow C_2H_3+H_2$	$9 \times 10^{-10} \exp(-62.36/R/T_g)$	16
R93	$C_2H_4+H \rightarrow C_2H_5$	$9.68 \times 10^{-12} (T_g/298)^{1.28} \exp(-5.4/R/T_g)$	16
R94	$2C_2H_3 \rightarrow C_2H_4+C_2H_2$	3.5×10^{-11}	16
R95	$C_2H_3+C_2H \rightarrow 2C_2H_2$	3.15×10^{-11}	16
R96	$C_2H_3+C_3H_8 \rightarrow C_2H_4+C_3H_7$	$1.46 \times 10^{-13} (T_g/298)^{3.3} \exp(-43.9/R/T_g)$	16
R97	$C_2H_3+C_3H_7 \rightarrow C_3H_8+C_2H_2$	2.01×10^{-12}	16
R98	$C_2H_3+C_3H_7 \rightarrow C_3H_6+C_2H_4$	2.01×10^{-12}	16
R99	$C_2H_3+C_3H_6 \rightarrow C_3H_5+C_2H_4$	$1.68 \times 10^{-15} (T_g/298)^{3.5} \exp(-19.62/R/T_g)$	16
R100	$C_2H_3+C_3H_5 \rightarrow C_3H_6+C_2H_2$	8×10^{-12}	16
R101	$C_2H_3+H_2 \rightarrow C_2H_4+H$	$1.61 \times 10^{-13} (T_g/298)^{2.63} \exp(-35.75/R/T_g)$	16
R102	$C_2H_3+H \rightarrow C_2H_2+H_2$	1.6×10^{-10}	16
R103	$C_2H_3+H \rightarrow C_2H_4$	$1.01 \times 10^{-11} T_g^{0.27} \exp(-140.92/T_g)$	16
R104	$C_2H_2+H \rightarrow C_2H+H_2$	$1 \times 10^{-10} \exp(-93.12/R/T_g)$	16
R105	$C_2H_2+H \rightarrow C_2H_3$	$9.3 \times 10^{-12} \exp(-1207.85/T_g)$	14
R106	$2C_2H \rightarrow C_2H_2+C_2$	3.01×10^{-12}	16
R107	$C_2H+C_3H_8 \rightarrow C_2H_2+C_3H_7$	5.99×10^{-12}	16
R108	$C_2H+C_3H_7 \rightarrow C_3H_6+C_2H_2$	1×10^{-11}	16
R109	$C_2H+C_3H_6 \rightarrow C_3H_5+C_2H_2$	5.99×10^{-12}	16
R110	$C_2H+H_2 \rightarrow C_2H_2+H$	$9.43 \times 10^{-14} T_g^{0.9} \exp(-1003.02/R/T_g)$	16
R111	$C_2H+H \rightarrow C_2+H_2$	$5.99 \times 10^{-11} \exp(-118/R/T_g)$	16
R112	$C_2H+H \rightarrow C_2H_2$	1.66×10^{-7}	16
R113	$C_3H_8+C_3H_5 \rightarrow C_3H_6+C_3H_7$	$5.71 \times 10^{-14} (T_g/298)^{3.3} \exp(-83.06/R/T_g)$	16
R114	$C_3H_8+H \rightarrow C_3H_7+H_2$	$2.19 \times 10^{-18} T_g^{2.54} \exp(-3400.1/T_g)$	16
R115	$C_3H_7+C_3H_7 \rightarrow C_3H_6+C_3H_8$	2.81×10^{-12}	16
R116	$C_3H_7+C_3H_6 \rightarrow C_3H_5+C_3H_8$	$1.69 \times 10^{-15} (T_g/298)^{3.5} \exp(-27.77/R/T_g)$	16
R117	$C_3H_7+C_3H_5 \rightarrow C_3H_6+C_3H_6$	$2.41 \times 10^{-12} \exp(-0.55/R/T_g)$	16
R118	$C_3H_7+H_2 \rightarrow C_3H_8+H$	$3.19 \times 10^{-14} (T_g/298)^{2.84} \exp(-38.25/R/T_g)$	16
R119	$C_3H_7+H \rightarrow C_3H_6+H_2$	3.01×10^{-12}	16
R120	$C_3H_7+H \rightarrow C_3H_8$	6×10^{-11}	16
R121	$C_3H_6+H \rightarrow C_3H_5+H_2$	$4.4 \times 10^{-13} (T_g/298)^{2.5} \exp(-10.39/R/T_g)$	16
R122	$C_3H_6+H \rightarrow C_3H_7$	$1.29 \times 10^{-11} (T_g/298)^{0.51} \exp(-5.15/R/T_g)$	16
R123	$C_3H_5+H_2 \rightarrow C_3H_6+H$	$1.39 \times 10^{-13} (T_g/298)^{2.38} \exp(-79.49/R/T_g)$	16

R124	$C_3H_5+H\rightarrow C_3H_6$	$78.8\times(T_g/298)^{-11.76} \exp(-98.53/R/T_g)$	16
R125	$H+H+CH_4\rightarrow H_2+CH_4$	$5.52\times 10^{-30} T_g^{-1}$	16
R126	$CH_4\rightarrow CH_3+H$	$7.5\times 10^{-7} \exp(-380/R/T_g)$	16
R127	$CH_3\rightarrow CH_2+H$	$1.7\times 10^{-8} \exp(-379/R/T_g)$	16
R128	$CH_3\rightarrow CH+H_2$	$1.66\times 10^{-8} \exp(-357/R/T_g)$	14
R129	$CH_2\rightarrow CH+H$	$2.66\times 10^{-10} \exp(-268/R/T_g)$	16
R130	$CH_2\rightarrow C+H_2$	$9.33\times 10^{-9} \exp(-375/R/T_g)$	16
R131	$CH\rightarrow C+H$	$3.16\times 10^{-10} \exp(-280/R/T_g)$	16
R132	$C_2H_6\rightarrow M^c$	0.5	–

^a Rate coefficient are given in s^{-1} , $cm^3 s^{-1}$, and $cm^6 s^{-1}$ for unimolecular, two-body, and three-body reactions, respectively.

^b Gas temperature T_g is given in K. R is the gas constant ($8.314\times 10^{-3} kJ mol^{-1} K^{-1}$).

^c M represents the non-gas phase products. The reaction is actually a simplification of a series of processes that produce high-carbon hydrocarbons. The rate is assumed based on the experimental results.

Table S2. Comparison of CH₄ conversion and C₂ products selectivity over various catalysts for the nonoxidative conversion of CH₄.

Catalysts	Metal loading (wt. %)	Temperature (°C)	GHSV (CH ₄ cm ³ g ⁻¹ h ⁻¹)	CH ₄ conversion (%)	C ₂ selectivity (%) ^c	Reference
Plasma+0.5Pd/CeO ₂ ^a	0.5	800	9,800	2.7	47.4	This work
Plasma+0.5Pd/CeO ₂ ^a	0.5	900	9,800	5.2	18.0	This work
Plasma+0.5Pd/CeO ₂ ^b	0.5	980	9,800	23.6	10.8	This work
Fe@SiO ₂	0.5	950	4,300	8.1	40.9	17
Fe@SiO ₂	0.5	980	5,900	22	~45	17
Fe@SiO ₂	0.5	1,090	19,200	48.1	52.1	17
Pt ₁ @CeO ₂	0.5	900	60	7.5	98.4	18
Pt ₁ @CeO ₂	0.5	975	60	14.4	74.3	18
Pt ₁ @CeO ₂	0.5	1,000	60	23.1	66.7	18
Ni-P/SiO ₂	9.2	800	12,000	0.02	64.8	19
Ni-P/SiO ₂	9.2	850	12,000	0.08	99.9	19
Ni-P/SiO ₂	9.2	900	12,000	0.51	75.8	19
Ni-B/SiO ₂	9.2	900	6,000	8.8	24	19

^a The catalyst was assisted by plasma with the frequency of 1 kHz. ^b The catalyst was assisted by plasma with the frequency of 3 kHz. ^c C₂ products consisted of C₂H₆, C₂H₄ and C₂H₂.

Table S3. The mean crystallite sizes (d) of the samples before and after the reaction with or without plasma calculated by Scherrer equation.

Samples	CeO ₂	0.5Pd/CeO ₂ -fresh	0.5Pd/CeO ₂ -used	Plasma+0.5Pd/CeO ₂ -used
d_{CeO_2} (nm) ^a	8.8	24.9	12.8	20.4

^a Calculated by the Scherrer equation, applied to the (111) reflection of fluorite CeO₂.

Table S4. The CH₄ conversion, C & H equilibrium and selectivity of major products based on the experiment and kinetic modeling in plasma without catalyst.

	C(CH ₄) ^c	C balance ^d	H balance ^d	S(C ₂ H ₆) ^e	S(C ₂ H ₄) ^e	S(C ₂ H ₂) ^e	S(C ₃ H ₆) ^e	S(H ₂) ^e
Sim. ^a	2.8	98.6	99.0	23.5	23.0	1.9	2.8	33.2
Exp. ^b	3	98.3	98.7	19.5	18.5	3.4	1.9	31.5

^a Simulation; ^b Experiment; ^c CH₄ conversion, %; ^d %; ^e selectivity of the various products, %.

Table S5. The CH₄ conversion, C & H equilibrium and selectivity of major products based on the experiment and kinetic modeling in the blank reactor without catalyst and plasma.

	C(CH ₄) ^c	C balance ^d	H balance ^d	S(C ₂ H ₆) ^e	S(C ₂ H ₄) ^e	S(H ₂) ^e
Sim. ^a	0.79	99.3	99.5	10.2	1.6	25.1
Exp. ^b	0.76	99.3	99.5	5.4	1.0	25.1

^a Simulation; ^b Experiment; ^c CH₄ conversion, %; ^d %; ^e selectivity of the various products, %.

References

- 1 H. Mai, L. Sun, Y. Zhang, R. Si, W. Feng, H. Zhang, H. Liu and C. Yan, *J. Phys. Chem. B*, 2005, **109**, 24380–24385.
- 2 H. Jeong, J. Bae, J. W. Han and H. Lee, *ACS Catal.*, 2017, **7**, 7097–7105.
- 3 Y. Gao, L. Dou, S. Zhang, L. Zong, J. Pan, X. Hu, H. Sun, K. Ostrikov and T. Shao, *Chem. Eng. J.* 2021, **420**, 127693.
- 4 Y. Gao, S. Zhang, H. Sun, R. Wang, X. Tu and T. Shao, *Appl. Energ.*, 2018, **226**, 534–545.
- 5 X. Hu, X. Fu, W. Wang, X. Wang, K. Wu, R. Si, C. Ma, C. Jia and C. Yan, *Appl. Catal. B*, 2020, **268**, 118424.
- 6 Z. Hu, X. Liu, D. Meng, Y. Guo, Y. Guo and G. Lu, *ACS Catal.*, 2016, **6**, 2265–2279.
- 7 G. Wang, M. Meng, Y. Zha and T. Ding, *Fuel*, 2010, **89**, 2244–2251.
- 8 G. Ercolino, P. Stelmachowski, G. Grzybek, A. Kotarba and S. Specchia, *Appl. Catal. B*, 2017, **206**, 712–725.
- 9 S. Lin, L. Yang, X. Yang and R. Zhou, *Appl. Surf. Sci.*, 2014, **305**, 642–649.
- 10 H. Huang, Q. Dai and X. Wang, *Appl. Catal. B*, 2014, **158–159**, 96–105.
- 11 F. Wang, C. Li, X. Zhang, M. Wei, D. G. Evans and X. Duan, *J. Catal.*, 2015, **329**, 177–186.
- 12 X. Wang, Y. Gao, S. Zhang, H. Sun, J. Li and T. Shao, *Appl. Energ.*, 2019, **243**, 132–144.
- 13 S. Zhang, Y. Gao, H. Sun, H. Bai, R. Wang and T. Shao, *J. Phys. D: Appl. Phys.*, 2018, **51**, 274005.
- 14 R. K. Janev and D. Reiter, *Phys. Plasmas*, 2002, **9**, 4071–4081.
- 15 R. K. Janev and D. Reiter, *Phys. Plasmas*, 2004, **11**, 780–829.
- 16 S. Heijkers, M. Aghaei and A. Bogaerts, *J. Phys. Chem. C*, 2020, **124**, 7016–7030.
- 17 X. Guo, G. Fang, G. Li, H. Ma, H. Fan, L. Yu, C. Ma, X. Wu, D. Deng, M. Wei, D. Tan, R. Si, S. Zhang, J. Li, L. Sun, Z. Tang, X. Pan and X. Bao, *Science*, 2014, **344**, 616–619.
- 18 P. Xie, T. Pu, A. Nie, S. Hwang, S. C. Purdy, W. Yu, D. Su, J. T. Miller and C. Wang, *ACS Catal.*, 2018, **8**, 4044–4048.
- 19 A. L. Dipu, S. Ohbuchi, Y. Nishikawa, S. Iguchi, H. Ogihara and I. Yamanaka, *ACS Catal.*, 2019, **10**, 375–379.